Jump Contagion among Stock Market Indices: Evidence from Option Markets

September 10, 2024

Abstract

We analyze the contagious propagation of jumps among international stock market indices, using a rich panel of high-frequency stock and options data (692,892 option contracts) over the period 2006–2015. We propose a multivariate option pricing model designed to allow for time and space amplification of jumps in option markets. We develop a semi-parametric estimation procedure, which employs a continuum of moment conditions in GMM with implied states and non-parametric high-frequency spot volatility estimation. A partial-information approach is introduced to reduce the computational complexity arising in the multivariate setting. Asymptotic properties of our estimators are derived and their finite-sample performance is analyzed. We find statistical evidence of jump contagion both within and between stock market indices. Our results reveal that jump contagion from the US to the UK is more pronounced than *vice versa*, whereas the jump contagion effects between the US and Germany stand on equal footing. We illustrate the statistical and economic importance of capturing jump contagion for risk management, option pricing, and scenario analysis. We show that accounting for jump contagion, employing scenarios based on the Global Financial Crisis, leads to an increase of capital requirements in the UK from 6% to 9% for each unit invested.

1 Introduction

Intricate linkages exist between international financial markets. Shocks to financial markets tend to propagate rapidly from one market to the next, potentially amplifying the initial shock via dynamic feedback loops. Such contagious amplification over time and in space (across markets) has important implications for risk management and scenario analysis, valuation and hedging, and portfolio choice and international diversification.

Option markets provide a unique laboratory to analyze these contagion effects. A panel of option price data, observed over time for different markets, strike prices (i.e., exercise prices) and maturities (i.e., expiry dates), embeds a wealth of information on the persistence, direction, and contagious nature of shocks.[1] Figure 1 provides an example of the propagation of shocks among the US (S&P 500) and UK (FTSE 100) option markets at the peak of the Global Financial Crisis of 2008. Panel (a) illustrates the interplay between the cascades of declines in the two underlying stock indices, starting with the initial drop in the US; and Panel (b) shows the reflection in option-implied volatilities for the two markets. The figures visualize in particular that the implied volatility slice for short maturity options on the UK index catches up with the US implied volatility counterpart by October 8, 2008, and even outruns it in terms of its steepness by the end of what constitutes the worst week in US stock markets since 1929.

Extracting time and space amplification features from options panels, however, constitutes a challenging statistical problem. This applies in particular to jump contagion, which refers to possibly asymmetric, feedback amplification effects between large moves in asset markets, leading to jump clusters in time and space. The challenges arise from the latency of the state variables—jump intensities and stochastic volatilities—in option pricing; the multitude of dimensions—time-series, maturity, moneyness (i.e., strike-to-price ratio) and
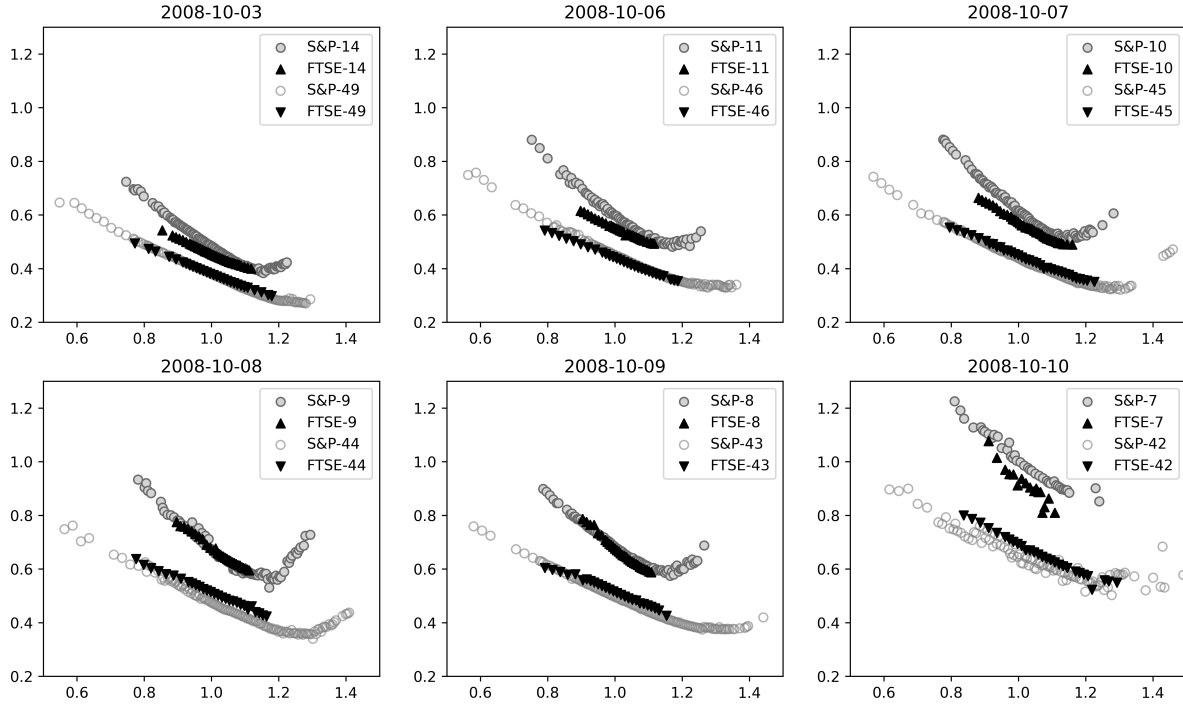
---

[1]For standard options terminology used in the sequel, we refer to the glossary in Hull (2021).

Figure 1: Contagion among the US and UK option markets, October 3–10, 2008

(a) Stock market indices
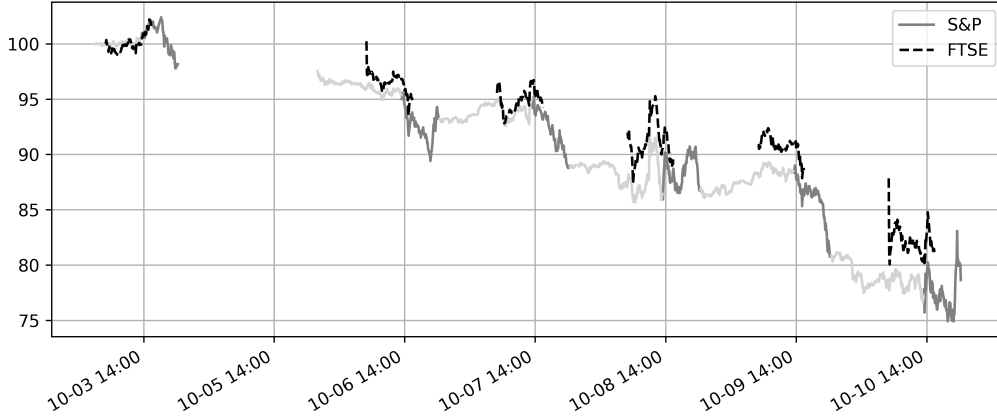
(b) Option-implied volatilities

Note: Panel (a) plots the E-Mini S&P 500 stock market futures index (S&P) and the FTSE 100 stock market index (FTSE), both scaled to 100 at the start of the sample. The observation frequency is 5 minutes, and trading times are converted to UTC (coordinated universal time), with October 4, 2008 (Saturday) omitted from the timeline. For the US futures index, the active trading periods (13:30–20:15 UTC) are highlighted in dark gray, while the remaining trading times are displayed in light gray. Panel (b) plots short-maturity Black-Scholes implied volatilities for the E-Mini S&P 500 stock market futures index options (S&P) and the FTSE 100 stock market index options (FTSE), against the moneyness level (i.e., the strike-to-price ratio). The days to maturity is indicated in the legends. The option prices are collected in the interval 14:03–14:05 UTC. More details are provided in Section 3.

cross-sectional—that play a role; and the subtlety of the features—not just occurrence of but contagion among jumps—we wish to explore. In this paper, we develop a statistical approach that exploits a rich, laboriously constructed and synchronized, panel of stock and options data to estimate a multivariate option pricing model designed to allow for, but not superimpose, time and space amplification of jumps.

We formulate our model under both the physical and the risk-neutral probability measures. The risk-neutral specification enables us to infer the unobserved state variables of our model by implying the parameter-dependent latent state variables from the panel of option prices. These are ingredients in an implied-state GMM approach with a *continuum* of moments (C-GMM) to identify the parametric components of our multivariate semi-martingale model—the drift and jump components. We treat the time-varying spot volatility components non-parametrically, by equating them to jump-robust estimates obtained from high-frequency data over short periods of time to facilitate robust identification of our rich model. This allows us to study, as is typical in classical GMM, a partially specified parametric model that only delineates a subset of statistical relationships that are of particular interest, while benefiting from the efficiency advantages of C-GMM. To reduce the computational complexity of the method, we introduce a partial-information approach, somewhat similar to the limited-information estimators considered by Singleton (2001). We analyze the asymptotic properties of our partial-information implied-state C-GMM procedure, and provide standard errors that account for the effect of implied-state moments on estimation uncertainty. Monte Carlo simulations indicate that our criterion function embodies sufficient information to identify the model parameters, yielding a good finite-sample performance.

We use these statistical tools to analyze a panel of high-frequency stock and options data for the UK (FTSE 100), Germany (DAX 30) and the US (S&P 500), covering January 2006 to August 2015 and containing 692,892 option contracts. Our findings can be sum-

4

marized as follows. First, we find significant evidence of both time and space amplification of jumps for all three markets. Second, our results reveal that jump contagion from the US to the UK is more pronounced than *vice versa*, in agreement with conventional wisdom that the US plays a "leading role" in international financial markets. Third, we find that jump contagion among the US and Germany is on equal footing for both markets. This remarkable finding may be explained by the fact that the German index serves as a proxy for the broader Eurozone market, which has played an important role in the financial crises of the decade we analyze. Furthermore, we demonstrate the statistical and economic importance of jump contagion in risk characteristics of log-return distributions, prices of multi-index options, and implied volatility dynamics for the S&P 500 and FTSE 100. We show e.g., that, when translated into capital requirements, accounting for jump contagion, using scenarios based on the Global Financial Crisis, amounts to an increase in required capital from 6% to 9% for each unit invested in the FTSE 100 index.

Our work is related to the literature studying the international transmission of equity shocks in the form of jumps, which is relatively small compared to the vast literature on international asset return and volatility spillovers; see Aït-Sahalia, Cacho-Diaz, and Laeven (2015), and also Errais, Giesecke, and Goldberg (2010) and Aït-Sahalia, Laeven, and Pelizzon (2014) who analyze jump contagion in credit defaults. High-frequency tests for common or mutually exciting jumps are developed in Jacod and Todorov (2009) and Dungey, Erdemlioglu, Matei, and Yang (2018); see also Aït-Sahalia and Xiu (2016). An even smaller literature—most closely related to our work—analyzes jump propagation through the lens of option markets. Andersen, Fusari, and Todorov (2020) consider the pricing of index options in separate markets, and find a large coherence across markets with respect to their left tail risk. Bakshi, Carr, and Wu (2008) investigate a genuinely multi-country stochastic discount factor using currency options, allowing for global and country-specific diffusion and jump risk factors. Kokholm (2016) considers a multivariate option pricing

model with a self- and/or cross-exciting jump component, under a risk-neutral specification. He applies it to sectoral indices in one market using a calibration technique. To our best knowledge, this paper is the first to analyze jump contagion among international stock market indices using the laboratory of option panel data.

Our statistical approach is inspired by the option-implied-state GMM approach of Pan (2002), and the C-GMM approach of Carrasco and Florens (2000, 2002) and Carrasco, Chernov, Florens, and Ghysels (2007). Different from this existing literature, our approach is semi-parametric in nature, mitigates the computational complexity of multivariate C-GMM using a partial-information approach, and takes estimation uncertainty from state-implied moments into account both formally in asymptotic analysis and numerically when computing standard errors.

This paper is organized as follows. Section 2 describes the model. Section 3 describes the data. Section 4 develops the estimation procedure. In Section 5 we present our empirical analysis. Conclusions are in Section 6. Further details on the model specification, data selection and processing, the estimation procedure, and data analysis are provided in four online appendices provided as supplementary material. Computer code to implement the procedures developed in this paper is available from a GitHub repository.[2]

2   Model Specification

This section presents our multivariate continuous-time option pricing model with contagious time and space amplification. It embeds the mutually exciting jump process proposed in Aït-Sahalia et al. (2015) to characterize the stock index dynamics in m economies. Unlike contagion models of multivariate stock index returns, modeling contagion among option prices requires extension of the pricing kernel. Therefore, we propose a class of

---

[2]`https://github.com/evladimirov/Jump-Contagion/`.

country-level risk-neutral probability measures that jointly accommodate arbitrage-free international stock price dynamics with mutually exciting jumps. Next, we describe the semi-nonparametric approximation adopted in our model.

2.1   Index Return Dynamics and Risk-Neutral Measures

We fix a filtered probability space $(\Omega, \mathcal{F}, \{\mathcal{F}_t\}_{t \geq 0}, \mathbb{P})$ and consider a model of index return dynamics for m economies equipped with mutually exciting jump processes. We assume that each of the markets is characterized by a stock market index denominated in the local currency with the following dynamics:

$$\frac{dS_{i,t}}{S_{i,t}} = \left(r_{i,t} - q_{i,t} + \eta_i \xi_{i,t}^2 + (\mathbb{E}[J_i] - \mathbb{E}^{\mathbb{Q}_i}[J_i])\lambda_{i,t}\right) dt + \xi_{i,t} dW_{i,t} + J_{i,t} dN_{i,t} - \mathbb{E}[J_i]\lambda_{i,t} dt, \quad (1)$$

for $i = 1, \ldots, m$, where $r_{i,t}$ and $q_{i,t}$ are deterministic risk-free rates and dividend yields; $W_{i,t}$ are standard Brownian motions, correlated with (possibly time-varying) pairwise instantaneous correlation coefficients $\varrho_{ij,t}$; $\xi_{i,t}$ are general, adapted volatility processes; and $J_{i,t} dN_{i,t}$ are compound Hawkes jump processes with serially and cross-sectionally independent random variables $J_{i,t}$ governing the jump sizes, having generic law F_{J_i} and mean $\mathbb{E}[J_i]$ (under $\mathbb{P}$). By $\mathbb{E}^{\mathbb{Q}_i}[J_i]$ we denote the expected jump size in market i under the equivalent risk-neutral probability measure $\mathbb{Q}_i$ specific to market i, as defined below. Throughout, stochastic processes, expectation operators, and parameters without superscript are understood to be defined with respect to the physical probability measure $\mathbb{P}$.

The Hawkes (1971) jump process, also known as the mutually exciting jump process, is a main ingredient of our model, allowing us to capture both jump contagion across markets and clustering of jumps in time within each market.[3] More specifically, we define

---

[3]Originally proposed to model epidemics, Hawkes processes have also been used to model seismic excitation since Ogata (1988).

the multivariate Hawkes jump process through m counting processes $N_{i,t}$, one for each of the m markets, such that each counting process is characterized by its conditional jump intensity process $\lambda_{i,t}$, defined by

$$\lambda_{i,t} = \lim_{s \downarrow 0} \frac{\mathbb{E}\left[N_{i,t+s} - N_{i,t} | \mathcal{F}_{t-}\right]}{s}. \tag{2}$$

Unlike the Poisson process, the jump intensity of the Hawkes process is stochastic with dynamics (under exponential decay) given by

$$d\lambda_{i,t} = \kappa_i(\overline{\lambda}_i - \lambda_{i,t})dt + \sum_{j=1}^{m} \delta_{ij} dN_{j,t}, \quad i = 1, \ldots, m. \tag{3}$$

In this specification, a jump event in equity index j causes the intensity $\lambda_{i,t}$ to increase by $\delta_{ij} \geq 0$, followed by an exponential decay towards $\overline{\lambda}_i > 0$ at a rate $\kappa_i > 0$. The parameters δ_{ij} dictate the *self-excitation* (for $i = j$) and *cross-excitation* (for $i \neq j$) effects, generating two key features of the model: first, a jump event increases the probability of subsequent jump events in the same index, leading to jump clustering in time; second, a jump event in one market increases the probability of jumps in other markets, entailing jump propagation in space. Note that, following a jump event in one market, the jump intensities in other markets respond instantaneously, thereby directly making jumps much more likely. Note also that these time and space amplification features are probabilistic and not superimposed, i.e., not certain to occur. The paired vectors (N, λ) jointly constitute a Markov process.

Our model captures jump contagion, i.e., the propagation over time and across markets of large moves in stock market indices. Sample paths from the model may exhibit nearly concurrent jumps in the different markets. By design, the model does not allow for large common exogenous shocks (it does allow for Brownian correlation), in line with the existing

literature on "contagion" in economics and finance as "propagation" rather than common shocks. Information, also common exogenous information, needs time to spread and get reflected in the different markets. Our model captures these cascading effects. To distinguish in formal statistical tests between contagious jumps and large common exogenous shocks would require a different modeling framework and ultra-high-frequency analysis.

In addition to the risk-free interest rate $r_{i,t}$ and dividend yield $q_{i,t}$ in economy i, the drift term in (1) contains two risk-premium components. The diffusive risk premium $\eta_i \xi_{i,t}^2$ is akin to the risk-return trade-off occurring in the capital asset pricing model (CAPM): η_i represents the additional expected return per unit of diffusive ("Brownian") variance $\xi_{i,t}^2$. The jump risk premium $(\mathbb{E}[J_i] - \mathbb{E}^{\mathbb{Q}_i}[J_i])\lambda_{i,t}$ represents the additional expected return under the physical measure (relative to the risk-neutral measure), needed to compensate for bearing jump risk. The last term in (1) is the compensator for the jump component; the compensated jump component is a local martingale. Our model specification allows for, possibly time-varying, correlations between the Brownian motions. However, in the presence of mutually exciting jumps, the contribution of the Brownian correlation to the realized correlation is swamped in crisis episodes, even if the Brownian correlation increases during such time periods, and therefore it plays only a secondary role.

As is common in the literature (e.g., Pan (2002), Broadie, Chernov, and Johannes (2007)), we assume the relative jump sizes $J_{i,t}$, $i = 1, \ldots, m$ to be independent log-normal random variables. Specifically, conditional upon a jump event in market i, the equity price jumps from $S_{i,t-}$ to $S_{i,t} = S_{i,t-}\exp(Z_{i,t})$, with $Z_{i,t} \sim \mathcal{N}(\mu_i, \sigma_i^2)$. Under this parametrization, the relative jump size in index i is $J_{i,t} = \exp(Z_{i,t}) - 1$, with mean $\mathbb{E}[J_{i,t}] = \exp(\mu_i + \frac{1}{2}\sigma_i^2) - 1$. When the mean parameters (i.e., μ_i) are estimated at negative values, as is the case in our data analysis, this entails that negative jumps in our model occur more frequently, and are more contagious, than positive jumps. We also assume that the vector of stacked jump sizes Z_t, vector of Brownian motions W_t, and vector of jump processes

9

N_t are mutually independent. Importantly, this model admits a generalized affine jump-diffusion representation as defined in Appendix B of Duffie, Pan, and Singleton (2000).

The sources of uncertainty stemming from the random jumps in our model render each market i, consisting of the equity index, a finite number of options on that index and a money market account, incomplete. Therefore, the stochastic discount factor for each of the markets is not unique. To formulate our risk-neutral pricing model, we focus on candidate pricing kernels that keep the joint dynamics of the log-equity index and the jump intensity process for each market i, under the equivalent risk-neutral probability measure $\mathbb{Q}_i$, within the generalized affine jump-diffusion class. We provide further details on the measure change in Appendix A.1, formally establishing in particular that the pricing kernels thus specified rule out arbitrage opportunities within each market as well as internationally.

The resulting model under $\mathbb{Q}_i$ may be represented as

$$\frac{dS_{i,t}}{S_{i,t}} = (r_{i,t} - q_{i,t})\, dt + \xi_{i,t} dW_{i,t}^{\mathbb{Q}_i} + J_{i,t} dN_{i,t} - \mathbb{E}^{\mathbb{Q}_i}[J_i]\lambda_{i,t} dt, \tag{4}$$

for $i = 1, \ldots, m$, where $dW_{i,t}^{\mathbb{Q}_i} = dW_{i,t} + \eta_i \xi_{i,t} dt$, with $W_{i,t}^{\mathbb{Q}_i}$ a standard Brownian motion under $\mathbb{Q}_i$. The pairwise instantaneous correlation coefficients $\varrho_{ij,t}$ between the Brownian motions are preserved under each of the risk-neutral measures. The distribution of the jump size random variables $J_{i,t} = e^{Z_{i,t}} - 1$ is of the same translated log-normal type under $\mathbb{Q}_i$ as under $\mathbb{P}$, but with possibly different parameters. We assume that only the mean parameters are different under the physical and risk-neutral specifications, i.e., $\sigma_i^{\mathbb{Q}_i} \equiv \sigma_i$, as in the univariate model of Pan (2002). The assumption of equal jump size variances under both measures is needed for the identification of the jump size parameters. As a consequence, the jump risk premium $(\mathbb{E}[J_i] - \mathbb{E}^{\mathbb{Q}_i}[J_i])\lambda_{i,t}$ is generated by the difference between μ_i and $\mu_i^{\mathbb{Q}_i}$.[4]

---

[4]Our specification of the pricing kernel sets the jump-timing risk premium to zero, so that the dynamics of the jump intensity processes in (3), and in particular the parameters κ_i, $\bar{\lambda}_i$ and δ_{ij}, are the same under

2.2 Semi-Nonparametric Approximate Index Return Dynamics

In the formulation of the model, the diffusive volatility processes $\xi_{i,t}$ have not yet been specified. In principle, they could be modelled using a parametric stochastic volatility specification. Alternatively, we adopt a semi-nonparametric approximation for the index return dynamics using nonparametric estimates of the spot volatilities $\xi_{i,t}$. Such an approximation leads to robust pricing of close-to-maturity options, allowing inference to be focused on the latent jump intensity dynamics and jump sizes. Moreover, a fully parametric version of the model, including a stochastic volatility specification, is prone to model misspecification and identification problems, especially in a multivariate setting; the semi-nonparametric approach considerably reduces these complications.

As in the univariate setting of Andersen, Fusari, and Todorov (2017), we use an approximate representation of the stock index process with constant spot volatility and a constant dividend yield and interest rate. Under the equivalent martingale measures $\mathbb{Q}_i$, we define the approximate processes $\tilde{S}_{i,s}^{\mathbb{Q}_i}, i = 1, \ldots, m$ for $s \in [t, T]$ (the time period between pricing and expiration of the option) as follows:

$$
\begin{cases}
\dfrac{d\tilde{S}_{i,s}^{\mathbb{Q}_i}}{\tilde{S}_{i,s}^{\mathbb{Q}_i}} = (r_{i,t} - q_{i,t})ds + v_{i,s}dW_{i,s}^{\mathbb{Q}_i} + J_{i,s}dN_{i,s} - \mathbb{E}^{\mathbb{Q}_i}[J_i]\lambda_{i,s}ds, & s \in [t, T], \\[2mm]
v_{i,s} = \xi_{i,t}\mathbb{1}_{\{t \le s \le T\}}, \qquad \tilde{S}_{i,t}^{\mathbb{Q}_i} = S_{i,t}.
\end{cases}
\tag{5}
$$

In other words, the spot volatility $v_{i,s}$ is taken to be constant and equal to $\xi_{i,t}$ (the true spot volatility at time t) over the interval $s \in [t, T]$, and the approximate process $\tilde{S}_{i,s}^{\mathbb{Q}_i}$ is initialized at the true index price $S_{i,t}$ at time t. We also refer to the insightful work of Medvedev and Scaillet (2007, 2010), who consider a small time-to-maturity asymptotic approximation of the implied volatility function for stochastic volatility jump-diffusions.

This approximation is reasonable for pricing short-dated options because under the

$\mathbb{P}$ and $\mathbb{Q}_i$; see Appendix A.1 for details.

risk-neutral measures, the stochastic volatility process usually exhibits slow mean reversion. For example, Pan (2002) finds the mean-reversion parameter in the volatility process to be 0.013 under $\mathbb{Q}$, expressed in daily terms, corresponding to a one-day autocorrelation coefficient in volatility equal to 0.987. Moreover, as close-to-maturity European-style option prices are more sensitive to the specification of the jump intensity dynamics and of the jump size distribution, pricing these options using the approximated process $\tilde{S}_{i,t}^{\mathbb{Q}_i}$ instead of $S_{i,t}$ leads to negligible approximation errors. We confirm this in simulations in Section 4.3 and Appendix C.4. Unlike Andersen et al. (2017) we do not "freeze" the jump intensity to its value at time t, because in our setting it can vary considerably, even over the short period, due to the self-excitation and contagion effects discussed in Section 2.1.

Finally, as the change of measure does not affect the diffusion term of the price dynamics, we can also adopt the approximate dynamics for the processes under $\mathbb{P}$:

$$
\begin{cases}
\dfrac{d\tilde{S}_{i,s}}{\tilde{S}_{i,s}} = (r_{i,t} - q_{i,t} + \eta_i \xi_{i,t}^2)ds + v_{i,s}dW_{i,s} + J_{i,s}dN_{i,s} - \mathbb{E}^{\mathbb{Q}_i}[J_i]\lambda_{i,s}ds, \qquad s \in [t,T], \\
v_{i,s} = \xi_{i,t}\mathbb{1}_{\{t \le s \le T\}}, \qquad \tilde{S}_{i,t} = S_{i,t},
\end{cases}
\tag{6}
$$

for $i = 1, \ldots, m$, but with $T = t + 1$; i.e., the spot volatility is assumed constant over the period of a single day. The specifications (5)–(6) will serve as a basis for the estimation procedure developed in Section 4.

3 The Data

Estimation is based on a rich panel of daily observations, which have, in turn, been constructed from tick-by-tick spot, futures and option price data for the FTSE 100, DAX 30 and S&P 500 stock market indices, spanning the period January 1, 2006, to August 13, 2015. That is, we exploit a very large sample of intra-day tick-by-tick observations to ob-

tain daily synchronized panels of options data for the three markets in the different time zones, as well as jump-robust spot volatility estimates constructed from intra-day returns in a time interval preceding the observation time of the options. The synchronicity of cross-market observations in our estimation sample is essential for capturing jump contagion among stock market indices. We then use the panel of daily data to estimate bivariate as well as univariate versions of the model. The sampling of tick-by-tick data underlying the option panel observations is a non-trivial task, which warrants further description. This section summarizes the data collection process; additional details are in Appendix B.

The data-set was obtained from the Thomson Reuters Tick History database, containing time-stamped tick-by-tick data from electronic exchanges for several major stock market indices and corresponding exchange-listed derivative contract prices. Data samples contain bid-ask quotes and transaction prices with time-stamps in the exchange's local time zone that denote the time at which the price data were received by Thomson Reuters from the exchange's servers. As the use of official exchange-determined "close" prices is not possible because the options are traded in different time zones, we use the synchronization procedure as outlined next.

We create daily option panels using tick-by-tick data subsets selected from a particular time interval during market trading hours, which we refer to as *reference interval*. We choose reference intervals for market pairs such that for each corresponding pair the trade recordings are as "synchronized" as possible to the right point of the reference interval, which we refer to as *reference point*. Throughout the sample we fix the reference interval for FTSE 100 options to 15:03–15:05 and for DAX 30 options to 16:03–16:05 (local exchange times). The reference interval for the S&P 500 options is obtained by translating the UK (and Germany) reference interval to US local exchange times using IANA Time Zone Database conventions, meaning option data for the US is usually sampled between 9:03–9:05 CST, with periodical exceptions dictated by daylight saving time adjustments used in

13

the US and in Europe. We impose several rules and filters in the data selection routine; see Appendix B.1 for specific details. Table 1 provides the descriptive statistics for the filtered option sample for each of the three markets. In Table B.1 in the appendix, we analyze the sensitivity to the choice of the reference intervals. Specifically, we analyze descriptive statistics for the filtered option sample using two-minutes and increased five-minutes intervals. Whereas some differences between the two reference intervals are visible, they are rather marginal. Table 1, Panel D, shows that the bid-ask spreads are the smallest for S&P, while the spreads for DAX and FTSE are of a similar magnitude. Our estimation procedure relies on transaction data if available and otherwise on mid bid-ask quotes. The percentage of transaction data is typically less than 1% for all three markets and for different ranges of maturity and moneyness levels, as new quotes arrive much more frequently than actual trades occur. The minimum tick sizes are 0.05 (S&P), 0.1 (DAX) and 0.5 (FTSE). The data might be noisier in less liquid markets, although this is not visible in the sample standard deviations of implied volatility in Table 1, Panel C.

In addition to the filtered option data, we use short-term interbank lending interest rates for each relevant currency, which we interpolate to match option time-to-maturity. Specifically, we use LIBOR-US, LIBOR-GBP and EURIBOR short-term rates for options on S&P 500 futures, and the FTSE 100 and DAX 30 indices, respectively. We follow Aït-Sahalia and Lo (1998) by backing out forward prices from put-call parity pairs and estimating our model using log-forward returns, circumventing the need to specify and calibrate dividend yield dynamics. The details on forward price calculations are provided in Appendix B.2. We further interpolate the sample Black-Scholes implied volatilities over a fixed set of moneyness and option maturities to construct a (homogeneous) panel of input data for the estimation procedure. Interpolating implied volatilities is a common procedure; see, e.g., Broadie et al. (2007) and Bardgett, Gourier, and Leippold (2019). Details about the interpolation procedure we employ are provided in Appendix B.3. Finally, for the non-

Table 1: Descriptive statistics for the option implied volatility data

	FTSE 100		DAX 30		S&P 500	
	$5 < \tau \leq 40$	$40 < \tau \leq 75$	$5 < \tau \leq 40$	$40 < \tau \leq 75$	$5 < \tau \leq 40$	$40 < \tau \leq 75$
Panel A: Aggregate number of option contracts						
$0.75 < k \leq 0.85$	1,375	2,968	9,505	16,000	23,413	33,499
$0.85 < k \leq 0.92$	6,646	8,914	18,139	21,831	36,986	41,122
$0.92 < k \leq 0.98$	18,743	16,670	20,637	20,843	40,197	40,236
$0.98 < k \leq 1.03$	23,127	18,285	17,300	17,332	34,234	34,250
$1.03 < k \leq 1.10$	10,911	13,052	17,838	21,861	28,560	37,994
$1.10 < k \leq 1.20$	1,258	2,721	4,764	9,875	6,782	15,024
Total	62,060	62,610	88,183	107,742	170,172	202,125
Panel B: Sample mean of implied volatility (%)						
$0.75 < k \leq 0.85$	38.7	35.3	36.6	33.1	39.3	32.7
$0.85 < k \leq 0.92$	31.2	27.2	30.4	27.2	29.0	25.5
$0.92 < k \leq 0.98$	22.0	20.8	24.1	23.1	21.8	20.8
$0.98 < k \leq 1.03$	17.2	16.9	20.0	20.1	16.7	17.0
$1.03 < k \leq 1.10$	18.8	17.1	19.2	18.2	16.7	15.4
$1.10 < k \leq 1.20$	31.0	24.6	26.0	21.1	26.7	20.2
Total	21.2	20.6	25.1	23.8	24.1	22.0
Panel C: Sample standard deviation of implied volatility (%)						
$0.75 < k \leq 0.85$	9.8	10.6	7.0	7.4	10.6	8.6
$0.85 < k \leq 0.92$	10.9	8.9	8.4	7.3	9.0	7.7
$0.92 < k \leq 0.98$	8.7	7.6	7.9	7.1	8.5	7.6
$0.98 < k \leq 1.03$	7.9	6.9	7.9	7.0	8.5	7.6
$1.03 < k \leq 1.10$	9.2	7.6	7.8	6.7	8.8	7.6
$1.10 < k \leq 1.20$	11.6	9.9	9.8	7.9	11.4	8.8
Total	10.3	9.3	9.9	8.7	11.9	9.8
Panel D: Sample mean of bid-ask spread (local currency)						
$0.75 < k \leq 0.85$	2.52	3.44	3.12	3.18	0.25	0.33
$0.85 < k \leq 0.92$	2.32	2.83	2.60	2.62	0.26	0.44
$0.92 < k \leq 0.98$	2.22	2.94	2.03	2.70	0.38	0.60
$0.98 < k \leq 1.03$	2.62	3.35	2.84	3.52	0.50	0.68
$1.03 < k \leq 1.10$	2.41	2.76	2.75	2.60	0.30	0.48
$1.10 < k \leq 1.20$	3.50	3.74	4.09	3.37	0.41	0.52
Total	2.45	3.09	2.70	2.97	0.35	0.50

This table provides descriptive statistics for filtered option data on FTSE 100, DAX 30 and S&P 500 futures. The sample contains daily option data from January 1, 2006, to August 13, 2015. The filters employed in the data selection procedure are detailed in Appendix B.1. Observations are bucketed into two categories for time-to-maturity, τ, and into six categories with respect to the moneyness level, defined as strike-to-forward ratio $k = K/F$.

parametric spot volatility estimates, we exploit high-frequency index return data. More specifically, to obtain spot volatility estimates, we use one-minute index return series[5]

---

[5]Non-parametric volatility estimates from one-minute returns are not systemically higher than those based on two- and five-minutes returns. Also, one-minute return series exhibit insignificant positive auto-correlation. These features suggest that microstructure noise is not strongly present in the return series.

from the beginning of each trading day until, but not including, the reference interval for each pair. Thus, the time periods used to obtain non-parametric volatility estimates do not overlap with the option recordings' time intervals, which allows us to use the model approximation proposed in Section 2.2.

4   Estimation Procedure

In this section, we develop the estimation procedure used for the data analysis. To obtain estimates of the spot volatility values $v_{i,t}$, we employ a jump-robust spot volatility estimator based on high-frequency returns observed before time t, with adaptive thresholding as in Bollerslev and Todorov (2011). Appendix C.1 provides details about this estimator. These estimators have been shown to be consistent under a typical in-fill asymptotic scheme, and to be robust in applications and in simulations. Given the spot volatility estimates, parameter estimation involves optimization of a GMM-type criterion function, the evaluation of which consists of two stages.

In the first stage, we back out the parameter-dependent jump intensities—the unobserved part of the state vector—using the option-pricing relation: as option prices are functions of the state variables, we can exploit this functional form to recover the latent states from the market observables, given a set of model parameter values. In the second stage, we evaluate the criterion function given this set of parameter values and the state vector consisting of observed index prices and implied jump intensities. The general method of using implied variables in a GMM-type estimation procedure was coined "implied-state GMM" by Pan (2002), who used *standard* GMM based on univariate option-implied volatilities.

In contrast to Pan (2002), we design an estimation procedure based on GMM with a *continuum* of moment conditions (C-GMM). C-GMM was initiated in the innovative work of Carrasco and Florens (2000, 2002), in a setting without latent states. The use of a

continuum of moments allows us to exploit more information than standard GMM with a finite number of moment conditions, which should result in more reliable and efficient estimates. That is, our point of departure is a novel combination of implied-state GMM and C-GMM. Beyond this combination, our methodological contribution is three-fold: (a) we develop a semi-parametric approach, which allows the parametric identification of jump contagion to be robust against misspecification of diffusive volatility; (b) we develop a partial-information version of implied-state C-GMM that mitigates the exponentially increasing computational complexity associated with larger-dimensional state vectors; and (c) we take estimation uncertainty from state-implied moments into account both formally in asymptotic analysis and numerically when computing (asymptotic or bootstrap) standard errors. These contributions demand an extension of the existing asymptotic theory for C-GMM, developed in the appendix. Our main contributions lie in the comprehensive data analysis. The semi-parametric approach requires a consistency result for non-parametric spot volatility estimation, available in the literature; our paper does not make a contribution to the specific spot volatility estimation literature. Throughout this section, we assume that for each of the markets $i = 1, \ldots, m$, and at regular-interval observation times $t = 0, 1, \ldots, T$, we observe a vector of (maturity- and moneyness-dependent) market-traded option prices $p_{i,t}$, the forward price on the index $F_{i,t}$, and the spot volatility estimate $\hat{v}_{i,t}$.

4.1 Implying the Latent States

The first stage in our estimation procedure consists of backing out the latent jump intensities from the option prices given a parameter vector θ. Let us define the option pricing relation determining a stacked vector of option prices $p_t = (p'_{1,t}, \ldots, p'_{m,t})'$, with $\tau_t = (\tau'_{1,t}, \ldots, \tau'_{m,t})'$ the corresponding time to maturity and $k_t = (k'_{1,t}, \ldots, k'_{m,t})'$ the moneyness level, given the vector of forward prices F_t and jump intensities λ_t, model parameters

θ, and volatility estimates $\hat{v}_t$, as follows:

$$p_t = \mathcal{P}(F_t, \lambda_t, \theta, \hat{v}_t, \tau_t, k_t), \qquad (7)$$

with $\mathcal{P} : \mathbb{R}_+^m \times \Lambda \times \Theta \times \mathbb{R}_+^m \times \mathbb{R}_+^{mn_\tau} \times \mathbb{R}_+^{mn_k} \to \mathbb{R}_+^{mn_\tau n_k}$. Here $\Lambda \subseteq \mathbb{R}_+^m$ is the domain of the jump intensities and Θ is a compact parameter space, such that the stationarity condition of the multivariate Hawkes process is satisfied. This requires the spectral radius of the matrix consisting of the entries (δ_{ij}/κ_i), $i, j = 1, 2$, to be less than unity. Note that we use several option prices with different characteristics at any time t and within any market i, i.e., $\tau_{i,t} \in \mathbb{R}_+^{n_\tau}$ and $k_{i,t} \in \mathbb{R}_+^{n_k}$, where n_τ and n_k represent the number of different maturities and moneyness levels, respectively.

We exploit the option-pricing relation (7) to imply the latent jump intensities. Formally, let us define the domain of invertibility of the option-pricing relation $\Sigma \subset \mathbb{R}_+^{mn_\tau n_k} \times \Theta \times \mathbb{R}_+^m \times \mathbb{R}_+^{mn_\tau} \times \mathbb{R}_+^{mn_k}$, such that it is a maximal set for which a mapping $f : \Sigma \to \Lambda$ is uniquely defined by

$$p_t = \mathcal{P}(F_t, f(p_t, F_t, \theta, \hat{v}_t, \tau_t, k_t), \theta, \hat{v}_t, \tau_t, k_t). \qquad (8)$$

Therefore, assuming that the inversion is well-defined, the option-implied jump intensities are defined by:

$$\lambda_t^\theta = f(p_t, F_t, \theta, \hat{v}_t, \tau_t, k_t), \qquad (9)$$

where we use the superscript θ to emphasize the dependence of the implied intensity on the parameter vector $\theta \in \Theta$, keeping in mind its dependence on the volatility estimates $\hat{v}_t$. Importantly, the vector of true intensities λ_t is retrieved based on the market-observables when evaluating the mapping (9) at the true model parameters θ_0 and using the true

volatility process ξ_t (assuming correct model specification).

We refer to Appendix C.2.1 for further details on implying the jump intensities. As discussed in Section 2.1, the model admits a generalized affine jump-diffusion representation under the physical and risk-neutral probability measures. One of the important advantages of the class of affine jump-diffusions is that the conditional characteristic function (CCF) of the state vector $X_T = (\log F_{1,T}, \ldots, \log F_{m,T}, \lambda_{1,T}, \ldots, \lambda_{m,T})'$ conditional on information available at time t is known in closed form (up to the solution of an ODE system) as an exponentially affine function of X_t; see Appendix A.2. This property is exploited in Appendix C.2.1 to obtain model prices.

After having implied the jump intensities we can construct a series of observations for the global state vector $X_t^\theta = (\log F_{1,t}, \ldots, \log F_{m,t}, \lambda_{1,t}^\theta, \ldots, \lambda_{m,t}^\theta)'$, which we then use in the criterion function evaluation, discussed in the following sub-section.

4.2 Parameter Estimation in a Full-Information Setting

In addition to obtaining option prices, the CCF also allows us to obtain the model-implied conditional density function of the state vector based on Fourier inversion, and thus, in principle, to employ classical maximum likelihood, which provides asymptotically efficient estimators (see, e.g., Singleton (2001)). However, Fourier inversion requires multivariate numerical integration at every time point, which is computationally highly expensive in an optimization routine. Singleton (2001) proposed to use method-of-moment estimators directly in the "frequency domain" using the CCF of a state vector. Such an estimator based on the CCF and its empirical counterpart avoids the need for Fourier inversion, thus it is computationally more appealing. Furthermore, Carrasco and Florens (2002) show that exploiting a continuum of moment conditions based on the CCF yields the asymptotic efficiency of maximum likelihood. We follow this route and develop, in our semi-parametric

setting, a C-GMM estimator that we extend to allow for implied state variables.

Because C-GMM requires a stationary Markovian state, we consider a state process $Y_t = (y_{1,t}, \ldots, y_{m,t}, \lambda_{1,t}, \ldots, \lambda_{m,t})'$, which consists of daily returns $y_{i,t} = \log F_{i,t} - \log F_{i,t-1}$ and latent jump intensities $\lambda_{i,t}$ for each of the markets. The CCF of the stationary state vector Y_{t+1} given the information at time t can be obtained from the CCF of the non-stationary state vector X_{t+1}:

$$\phi(s, Y_t, \Delta; \hat{v}_t, \theta) := \mathbb{E}\left[e^{\mathrm{i}s \cdot Y_{t+1}} | \mathcal{F}_t\right] = \mathbb{E}\left[e^{\mathrm{i}s \cdot X_{t+1}} | \mathcal{F}_t\right] e^{-\sum_{j=1}^m \mathrm{i}s_j \log F_{j,t}},$$

with Δ the sampling frequency of a single day. We consider the moment conditions based on the CCF of the state vector and its empirical counterpart. This involves combining the "raw" moment functions

$$u(s, Y_t, Y_{t+1}; \hat{v}_t, \theta) := e^{\mathrm{i}s \cdot Y_{t+1}} - \phi(s, Y_t, \Delta; \hat{v}_t, \theta), \tag{10}$$

with an instrument function $m(r, Y_t)$, to obtain the moment function

$$h(r, s, Y_t, Y_{t+1}; \hat{v}_t, \theta) := m(r, Y_t) \cdot u(s, Y_t, Y_{t+1}; \hat{v}_t, \theta) = m(r, Y_t)\left(e^{\mathrm{i}s \cdot Y_{t+1}} - \phi(s, Y_t, \Delta; \hat{v}_t, \theta)\right),$$

and hence the moment conditions

$$\mathbb{E}[h(r, s, Y_t, Y_{t+1}; \hat{v}_t, \theta_0)] = 0, \qquad \text{for all } r, s \in \mathbb{R}^{2m}. \tag{11}$$

The idea of GMM with a continuum of moments, developed in Carrasco and Florens (2000, 2002) and Carrasco et al. (2007), is to use not a discrete finite set of vectors s as arguments for the moment conditions (11), but rather to employ a full continuum of values of s. Furthermore, these authors show that also using a continuum of instruments of the

form $m(r, Y_t) = e^{\mathrm{i} r \cdot Y_t}$ with $r \in \mathbb{R}^{2m}$ leads to a considerable efficiency gain in estimation. We will adopt both elements in our estimation approach. Unlike the regular C-GMM set-up, not all components of the state vector Y_t are observed in our model. However, we can exploit the option-pricing relation (7) and imply the jump intensities from the market observables as discussed in the previous sub-section. Under some additional assumptions, formally stated later, we can use the moment conditions (11) based on the state vector with implied intensities $Y_t^\theta = (y_{1,t}, \ldots, y_{m,t}, \lambda_{1,t}^\theta, \ldots, \lambda_{m,t}^\theta)'$. Let us denote the sample analogue of the moment conditions (11) based on the state vector with implied intensities as

$$h_T(\tau; \hat{v}, \theta) := \frac{1}{T-1} \sum_{t=1}^{T-1} h(\tau, Y_t^\theta, Y_{t+1}^\theta; \hat{v}_t, \theta), \tag{12}$$

with $\tau = (r, s)' \in \mathbb{R}^{4m}$.

In Appendix C.2.2, we provide further details on the criterion function of the implied-state C-GMM procedure in the present 'full-information setting'. It turns out there that this procedure becomes computationally prohibitively expensive already for a bivariate model. We overcome this by developing a partial-information setting in the following sub-section.

4.3   Parameter Estimation in a Partial-Information Setting

Singleton (2001) notes that although full maximum likelihood (ML) estimation based on Fourier inversion of the CCF (ML-CCF) is computationally expensive in a multivariate setting, one could base estimation on the marginal conditional density functions $f(y_{i,t+1}|Y_t; \theta)$ of the single state variable $y_{i,t+1}$ conditional on the entire state vector Y_t. This limited-information (LML-CCF) approach requires at most N one-dimensional integrations for Fourier inversion instead of one N-dimensional integral evaluation. Therefore, a potential mild loss in asymptotic efficiency is traded off against the computational simplicity relative to the full ML-CCF approach.

A similar approach can be developed for the CCF-based C-GMM estimator, which allows us to considerably decrease the computational costs when focusing on the marginal CCF of a single economy. Therefore, instead of constructing the criterion function from one $2m$-dimensional integral as in (C.4), we exploit a partial-information estimator based on the sum of m^2 2-dimensional integrals. Although this approach can be described in the general multivariate setting, we apply it here to the bivariate model described in Appendix A.2, where we also provide the closed-form CCF for the bivariate model under $\mathbb{P}$.

Let us denote by $Y_t^{(1)} = (y_{1,t}, \lambda_{1,t})$ and $Y_t^{(2)} = (y_{2,t}, \lambda_{2,t})$ the *marginal market states* of the first and second economy, and by $Y_t^{(3)} = (y_{1,t}, \lambda_{2,t})$ and $Y_t^{(4)} = (y_{2,t}, \lambda_{1,t})$ the *marginal cross-market states*. Clearly, the marginal CCFs of the marginal states can be obtained from the joint CCF evaluated at the argument vectors $s^{(1)} := (s_1, 0, s_3, 0)'$, $s^{(2)} := (0, s_2, 0, s_4)'$, $s^{(3)} := (s_1, 0, 0, s_4)'$ and $s^{(4)} := (0, s_2, s_3, 0)'$, that is,

$$\phi^{(i)}\left(v, Y_t, \Delta; \hat{v}_t, \theta\right) := \phi\left(s^{(i)}, Y_t, \Delta; \hat{v}_t, \theta\right) = e^{\alpha^{(i)}(\Delta) + \beta_3^{(i)}(\Delta)\lambda_{1,t} + \beta_4^{(i)}(\Delta)\lambda_{2,t}}, \tag{13}$$

where $\alpha^{(i)}(\Delta), \beta_3^{(i)}(\Delta), \beta_4^{(i)}(\Delta)$ are the solutions to the ODE system (A.10) in Appendix A.2 solved with the initial values $s^{(i)}$ for $i = 1, 2, 3, 4$.

Similar to the general setting based on the joint CCF, we exploit the marginal CCFs to obtain the moment conditions. In the bivariate case, instead of the moment condition described in (11) we can consider four sets of "marginal" moment conditions stacked in a vector form, that is:

$$\mathbb{E}[\mathbf{h}(\tau, t; \theta_0)] = \mathbb{E}\left[\begin{pmatrix} h^{(1)}(\tau; \hat{v}_t, \theta_0) \\ h^{(2)}(\tau; \hat{v}_t, \theta_0) \\ h^{(3)}(\tau; \hat{v}_t, \theta_0) \\ h^{(4)}(\tau; \hat{v}_t, \theta_0) \end{pmatrix}\right] = \begin{pmatrix} 0 \\ 0 \\ 0 \\ 0 \end{pmatrix}, \tag{14}$$

22

with

$$h^{(i)}(\tau; \hat{v}_t, \theta) = m(r, Y_t^{(i)}) \left(e^{\mathrm{i} s \cdot Y_{t+1}^{(i)}} - \phi^{(i)}(s, Y_t; \hat{v}_t, \theta) \right),$$

where $i = 1, 2, 3, 4$, $\tau = (r, s)'$ and $r, s \in \mathbb{R}^2$.

In Appendix C.2.3, we provide additional details on the criterion function of this partial-information implied-state C-GMM procedure. Furthermore, we discuss in detail the asymptotic properties of this estimation procedure in Appendix C.3. More specifically, under Assumptions C.1–C.4 stated in the appendix—requiring stationarity and Markovianity of the process Y_t, regularity of the moment functions and their empirical counterparts, and consistency of the non-parametric spot volatility estimator—, we formally establish the asymptotic normality of our estimators and provide estimators for the asymptotic standard errors that account for the effect of implied-state moments.

To analyze the finite-sample performance of our estimation procedure, we provide detailed Monte Carlo simulation results in Appendix C.4. The results, a summary of which is contained in Table 2 with full details provided in the appendix, show a good finite-sample performance of our partial-information implied-state C-GMM procedure, notwithstanding the challenging nature of the statistical problem. We find in particular that the model parameters capturing jump contagion (i.e., κ_i, $\overline{\lambda}_i$, and δ_{ij}, $i, j = 1, 2$), which are of central interest in this paper, are identified with high precision. We note that our simulation design includes the semi-nonparametric approximation of Section 2.2 and the pricing errors induced by it. For comparison, Appendix C.4 also contains simulation results for (infeasible) moment conditions based on the fully parametric model assuming the spot volatilities and stochastic volatility parameters to be known. The results are similar, indicating that the "volatility freezing" approximation has relatively little effect on estimator behavior. Because the Monte Carlo analysis also shows that the asymptotic standard errors appear

Table 2: Monte Carlo simulation results for the bivariate model

	$\mu_1^{\mathbb{Q}_1}$	σ_1	κ_1	$\overline{\lambda}_1$	δ_{11}	δ_{12}	μ_1	η_1
true	-0.130	0.030	6.000	1.000	3.000	1.000	-0.040	2.000
25%	-0.133	0.027	5.520	0.924	2.685	0.925	-0.042	1.560
50%	-0.129	0.031	5.872	1.043	2.901	1.050	-0.038	2.467
75%	-0.125	0.034	6.116	1.086	3.070	1.131	-0.035	2.957
	$\mu_2^{\mathbb{Q}_2}$	σ_2	κ_2	$\overline{\lambda}_2$	δ_{22}	δ_{21}	μ_2	η_2
true	-0.130	0.030	5.000	1.000	2.000	3.000	-0.040	2.000
25%	-0.132	0.028	4.729	0.945	1.835	2.803	-0.043	1.333
50%	-0.127	0.030	4.925	1.083	2.002	3.074	-0.039	2.237
75%	-0.123	0.033	5.073	1.175	2.135	3.323	-0.036	2.667

This table summarizes the Monte Carlo simulation results of the partial-information implied-state C-GMM procedure. True parameters and Monte Carlo sample quantiles (at 25%, 50%, and 75%) are presented on separate rows. Further details are in Appendix C.4.

to be sensitive to the numerical implementation details of the relevant integrals, we will report, in the next section, bootstrap standard errors, using a parametric recursive-design bootstrap approach that is described in detail in Appendix C.5.

5 Data Analysis

In this section, we describe our estimation results for the three pairs of stock market indices we consider. We also provide three model applications to further highlight the statistical and economic importance of the jump cross-excitation effect.

5.1 Estimation Results

Parameter estimates for the bivariate models are displayed in Table 3. Each bivariate model is estimated using the partial-information implied-state C-GMM procedure developed in Section 4.3, using synchronized daily data for the corresponding stock market indices and their options panels following Section 3. The synchronicity between markets is crucial for

Table 3: Estimation results for FTSE 100, DAX 30 and S&P 500

	$\mu^{\mathbb{Q}}$	σ	κ	$\overline{\lambda}$	δ^s	δ^c	μ	η
FTSE	-0.126	0.020	4.063	0.353	1.638	2.506	-0.038	2.186
	[0.012]	[0.002]	[0.673]	[0.042]	[0.256]	[0.328]	[0.003]	[0.128]
DAX	-0.131	0.027	3.482	0.418	2.190	1.244	-0.025	2.680
	[0.011]	[0.003]	[0.671]	[0.044]	[0.283]	[0.196]	[0.002]	[0.168]
S&P	-0.148	0.036	3.320	0.296	2.501	0.517	-0.039	2.173
	[0.01]	[0.004]	[0.751]	[0.043]	[0.349]	[0.146]	[0.004]	[0.145]
FTSE	-0.131	0.033	3.216	0.283	1.709	2.119	-0.041	2.051
	[0.011]	[0.003]	[0.657]	[0.035]	[0.323]	[0.439]	[0.003]	[0.117]
S&P	-0.135	0.036	3.781	0.261	2.257	1.788	-0.037	1.977
	[0.016]	[0.005]	[0.749]	[0.05]	[0.273]	[0.263]	[0.006]	[0.285]
DAX	-0.138	0.039	4.235	0.394	2.287	1.658	-0.035	2.119
	[0.019]	[0.009]	[0.803]	[0.053]	[0.373]	[0.235]	[0.007]	[0.205]

This table reports bivariate model parameter estimates for three pairs of stock market indices: FTSE 100-DAX 30, S&P 500-FTSE 100, and S&P 500-DAX 30. The δ^s parameters capture self-excitation for each index based on pairwise estimation (i.e., $\delta_i^s = \delta_{ii}$, $i = 1, 2$), while the δ^c parameters capture cross-excitation for each pair (i.e., $\delta_i^c = \delta_{ij}$, $i, j = 1, 2$, $i \neq j$). Bootstrap standard errors are reported in square brackets.

the identification of jump contagion in space. We note that already in the bivariate setting, our model is a rich semi-parametric model with 16 parameters to be estimated. Whereas a trivariate analysis would be interesting and is theoretically feasible, it practically reaches the limits of what can be reliably identified in finite samples. This applies in particular to the self- and cross-excitation parameters, which increase from 4 to 9 when going from a bivariate to a trivariate analysis and which are of central interest in the paper.

The estimation results provide statistically significant evidence of both self- and cross-excitation in jumps for all three markets. According to our estimates, a single jump event leads to an increase in the corresponding own jump intensity ranging from $\delta^s = 1.6$ to 2.5 in the markets considered, given base rates $\overline{\lambda}$ ranging from 0.3 to 0.4. This self-excitation of jumps induces jump clustering in time.[6] Estimates of the cross-excitation parameter δ^c range from 0.5 to 2.5. From our cross-excitation estimates, we deduce that the UK market

---

[6]The self-excitation of jumps is broadly in line with the findings in Boswijk, Laeven, and Lalu (2015) and Du and Luo (2019), who studied univariate self-excitation models with parametric volatility dynamics in the US market index using weekly data.

is about four times as much exposed to shocks in the US market than *vice versa*. In other words, we observe a large asymmetry in the jump contagion among FTSE and S&P stock market indices, in line with conventional wisdom that the US market plays a leading role in international financial markets. On the other hand, cross-excitation in jumps between the US and German stock market indices is largely symmetric; in particular, the cross-excitation effect from Germany—perhaps as a proxy for the Eurozone economy of which the German economy accounts for nearly a third—to the US is stronger than suggested by conventional wisdom. The cross-excitation effect from DAX to FTSE has the largest cross-excitation parameter estimate. The reverse effect from FTSE to DAX is estimated to be twice as small. We find that the Wald tests for each pair of indices reject the null hypothesis that the cross-excitation parameters are equal to zero.[7]

Using the model parameter estimates in Table 3, we imply the latent jump intensities for each index from the corresponding sets of option prices. Figure 2 plots the implied jump intensities, along with the index log-forward returns. To back out the jump intensity for the UK stock market index we use the parameter estimates for the pair S&P-FTSE, while for the US and German markets we use the S&P-DAX pair estimates. We note that the jump intensity time series implied using parameter estimates from other pairs exhibit very similar dynamics with only minor differences in level. The jump intensities for all three markets follow a similar pattern: in our data sample, the time series of latent jump intensities backed out from option prices start at values close to the corresponding base rate intensities, spike in the fall of 2008 during the global financial crisis, increase during the European sovereign debt crisis, gradually decay towards the base rates after each of these events, and exhibit relatively stable dynamics afterwards.

---

[7]It is conceivable that markets with the richest option information (the US, and, to a lesser degree, Germany, see Table 1, Panel A) have the most pronounced (and most precise) estimation results. This difference between the three markets could be reduced by considering a subset of option contracts for a specific strike price range. This would, however, lead to such a loss of information that parameter identification would be jeopardized. In particular, identification of jump intensities and their dynamics requires option information over the full range of strike prices.
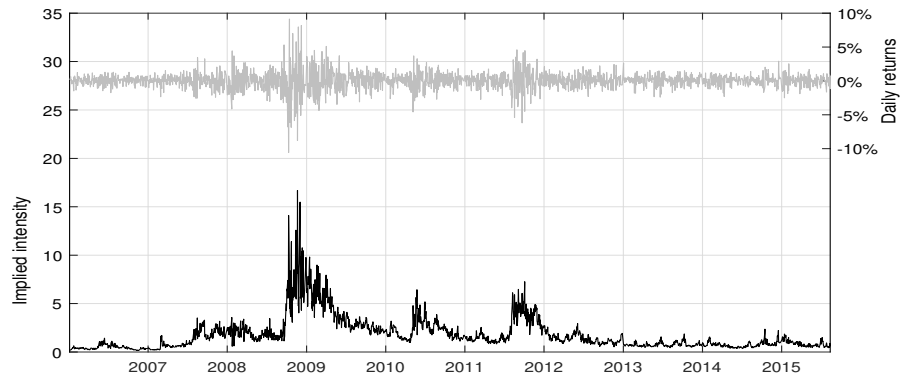
Figure 2: Time-series of the option-implied jump intensities
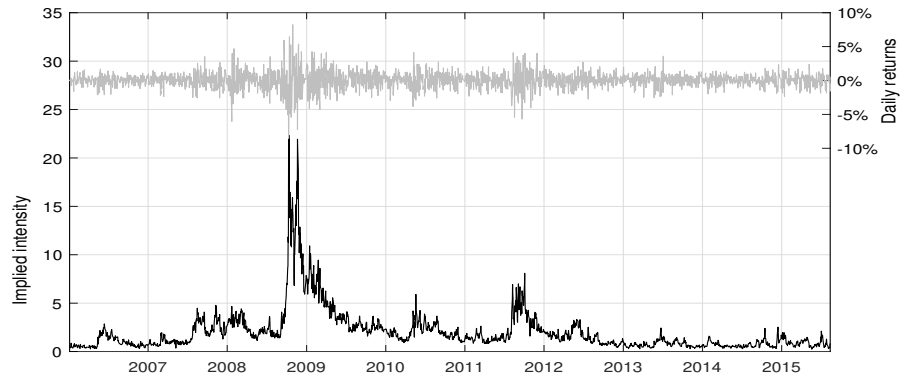
(a) FTSE 100
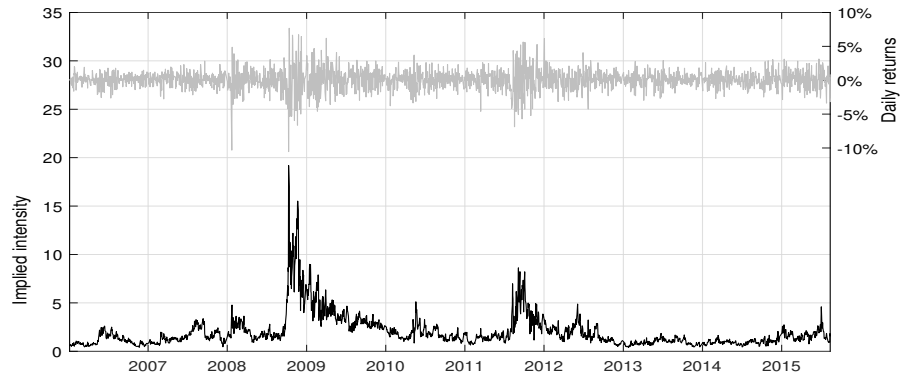
(b) DAX 30

(c) S&P 500

Note: This figure plots the time-series of option-implied jump intensities for FTSE 100, DAX 30 and S&P 500 stock market indices along with corresponding log-forward returns (secondary, right-hand axis in each subplot). The parameter estimates from the S&P-FTSE pair are used to imply the latent jump intensities for FTSE 100, while the estimates for the S&P-DAX pair are used to back out the jump intensities for DAX 30 and S&P 500.

Table 4: Option prices: Empirical fit

k	0.85	0.87	0.89	0.91	0.93	0.95	0.97	0.99	1.01	1.03	1.05	1.07	1.09	Total
FTSE.b	1.62	1.51	1.56	1.70	1.65	1.26	0.82	1.45	2.25	2.68	2.85	3.01	3.25	2.03
FTSE.u	1.75	1.57	1.52	1.62	1.61	1.36	1.13	1.66	2.38	2.84	3.11	3.40	3.71	2.20
S&P.b	1.82	1.76	1.77	1.73	1.47	0.98	0.95	1.86	2.55	2.81	2.96	3.24	3.76	2.26
S&P.u	1.96	1.95	1.92	1.76	1.39	1.02	1.51	2.50	3.04	3.15	3.21	3.42	3.94	2.50

This table reports the root mean square errors (RMSEs, displayed as a percentage) of the option prices written on the FTSE 100 and S&P 500 indices, expressed in terms of the market-observed and model-implied Black-Scholes implied volatility, as a function of the strike-to-forward ratio $k = K/F$, using the *bivariate* (.b) and *univariate* (.u) models and parameter estimates.

In our model set-up, the jump risk premia are driven by the difference in means between the jump sizes under the physical and risk-neutral probability measures, i.e., they are specified as $(\mathbb{E}[J] - \mathbb{E}^{\mathbb{Q}}[J])\lambda_t$ per unit of time. The estimated jump risk premium coefficients, $\mathbb{E}[J] - \mathbb{E}^{\mathbb{Q}}[J]$, for the bivariate models are around 8.0%, 9.0% and 9.5% for the UK, German and US stock market indices, respectively. We note that these coefficients are commensurate with the instantaneous level of the corresponding jump intensity process. Thus, the dynamics of the jump risk premia are time-varying and are increasing during turbulent periods together with the intensity processes.

To illustrate the empirical fit of the option prices that our model achieves, we display in Table 4 the root mean square errors (RMSEs) of the option prices. In particular, we consider the bivariate parameter estimates of the pair S&P-FTSE, and display the RMSEs obtained by comparing the market-observed and model-implied option prices. The table demonstrates that the model, estimated for the full sample spanning January 1, 2006, to August 13, 2015, fits well the observed option prices. The table also anticipates the (nearly uniformly positive) gains in fit of the bivariate model compared to its univariate counterpart discussed in the next subsection for both indices. In Appendix D.1, we also illustrate the empirical fit of the moment conditions within the partial-information implied-state C-GMM procedure. There, we also show that the parameter values, and the gains in fit of the bivariate model, are reasonably stable when estimated from a subsample.

Table 5: Univariate model estimation results for FTSE 100, DAX 30 and S&P 500

	$\mu^{\mathbb{Q}}$	σ	κ	$\overline{\lambda}$	δ	μ	η
FTSE	-0.127	0.030	2.132	0.318	1.798	-0.030	2.379
DAX	-0.137	0.032	3.207	0.486	2.132	-0.029	2.109
S&P	-0.161	0.043	2.445	0.305	2.176	-0.038	2.216

This table reports parameter estimates for the univariate model for FTSE 100, DAX 30 and S&P 500 stock market indices.

5.2   Applications

We illustrate the statistical and economic implications of jump contagion in three applications. In the classical GMM tradition, we provide throughout this subsection comparisons between parametric models that delineate only a subset of statistical relationships that are of particular interest. Specifically, we focus on the jump contagion channel that plays a central role in this paper. To gauge the effect of cross-excitation in the jump components across markets, we first provide estimation results for the univariate model specification. The univariate model can be seen as a nested version of the bivariate specification, in which the cross-excitation parameters are turned off. We note that for the estimation of the univariate model we use the same procedure: implied-state GMM with a continuum of moments as discussed in Section 4.2. The estimation results of the univariate models for the FTSE 100, DAX 30 and S&P 500 stock market indices are provided in Table 5. Turning off the cross-excitation channel in the jump component is likely compensated for by the other parameters of the model. For this reason we observe that, while the estimates for the remaining parameters are of the same magnitude, some differences should and do appear when comparing estimates between the univariate and bivariate models.

5.2.1   Distribution of Index Returns

As a first application, we consider the effect of jump contagion on the (conditional) distribution of index returns, under the physical probability measure $\mathbb{P}$ used for risk management.

Table 6: Descriptive statistics for the conditional log-return distribution (simulated using model parameter estimates, horizon $h = 10$ days)

	0.1%	1%	5%	25%	50%	75%	95%	S	K	$\mathbb{E}[N_t|\lambda_0]$
(a) Base Case: $\lambda_{1,0} = \overline{\lambda}_1, \lambda_{2,0} = \overline{\lambda}_2$										
Bivariate - FTSE	-7.47	-3.17	-2.10	-0.79	0.11	1.00	2.27	-0.52	6.27	0.0073
Univariate - FTSE	-6.34	-3.14	-2.10	-0.77	0.12	1.00	2.28	-0.28	4.46	0.0079
Bivariate - S&P	-7.90	-3.14	-2.08	-0.77	0.12	1.01	2.27	-0.59	7.17	0.0073
Univariate - S&P	-8.34	-3.13	-2.09	-0.76	0.13	1.02	2.30	-0.72	9.00	0.0079
(b) Euro Debt Crisis: $\lambda_{1,0} = \lambda_{2,0} = 5$										
Bivariate - FTSE	-12.98	-7.69	-3.09	0.32	1.36	2.33	3.68	-2.11	11.34	0.1249
Univariate - FTSE	-10.80	-6.26	-2.18	0.31	1.33	2.29	3.64	-1.72	10.03	0.1238
Bivariate - S&P	-13.29	-7.69	-2.71	0.50	1.53	2.49	3.84	-2.23	12.80	0.1242
Univariate - S&P	-14.27	-8.41	-2.50	0.67	1.68	2.64	4.02	-2.38	14.18	0.1206
(c) S&P Shock: $\lambda_{1,0} = 20, \lambda_{2,0} = \overline{\lambda}_2$										
Bivariate - FTSE	-9.56	-3.76	-2.07	-0.68	0.23	1.14	2.45	-1.00	9.04	0.0186
Univariate - FTSE	-6.66	-3.12	-2.10	-0.78	0.11	1.00	2.28	-0.39	5.85	0.0081
Bivariate - S&P	-15.88	-8.54	-2.99	3.79	5.89	7.10	8.76	-1.75	7.40	0.4872
Univariate - S&P	-16.63	-8.84	-3.01	4.54	6.57	7.78	9.65	-1.74	7.87	0.4872
(d) FTSE Shock: $\lambda_{1,0} = \overline{\lambda}_1, \lambda_{2,0} = 20$										
Bivariate - FTSE	-16.00	-9.14	-3.77	2.78	5.13	6.35	7.92	-1.73	7.08	0.4835
Univariate - FTSE	-12.29	-6.37	-2.10	3.33	5.15	6.34	7.97	-1.54	6.87	0.4924
Bivariate - S&P	-8.59	-3.22	-2.06	-0.74	0.15	1.05	2.33	-0.76	8.15	0.0104
Univariate - S&P	-7.83	-3.14	-2.07	-0.76	0.13	1.01	2.31	-0.58	8.19	0.0074
(e) 2008 Global Financial Crisis: $\lambda_{1,0} = 20, \lambda_{2,0} = 15$										
Bivariate - FTSE	-15.36	-8.89	-4.03	2.28	4.00	5.15	6.68	-1.83	7.72	0.3756
Univariate - FTSE	-11.83	-6.61	-2.55	2.45	3.89	4.99	6.53	-1.66	7.61	0.3693
Bivariate - S&P	-15.88	-8.54	-2.99	3.81	5.92	7.13	8.79	-1.75	7.38	0.4893
Univariate - S&P	-16.63	-8.85	-3.01	4.54	6.57	7.78	9.65	-1.74	7.87	0.4870

This table displays the empirical quantiles (in percentages), skewness (S), kurtosis (K), and expected number of jumps implied by the conditional distribution of simulated log-returns for S&P 500 ("index 1") and FTSE 100 ("index 2"). The stock index price paths are simulated using bivariate and univariate model parameter estimates, conditional upon different values ("scenarios") of the latent jump intensities. The return horizon is $h = 10$ days. Volatilities are assumed to be constant throughout the horizon and are set to $v_{i,s} = 8.36\%$ for both indices, and the instantaneous Brownian correlation is set to be 0.6.

For this purpose, we simulate forward prices for a pair of indices using the parameter estimates of the bivariate and univariate models from Tables 3 and 5, respectively. From the set of bivariate estimates, we use the S&P 500 and FTSE 100 parameter estimates; this pair exhibits the most pronounced jump contagion asymmetry according to our estimates.

Since the simulated distribution of log-returns is conditional on the (initial) jump intensity values, we consider five different scenarios to illustrate the effect of jump contagion.

Under the base scenario (a), the initial values of the intensities are given by the corresponding estimates of the base rates $\overline{\lambda}_1$ and $\overline{\lambda}_2$, while in scenarios (b)–(e) we assume the initial values to be similar to levels implied from our model during the 2008 Global Financial Crisis and the Euro Debt Crisis. Table 6 displays the empirical quantiles, skewness and kurtosis statistics as well as the expected number of jumps for the simulated log-return distributions under the bivariate and univariate models. The results are based on 100,000 random paths over a 10-day horizon simulated using an Euler scheme.

It is clearly apparent from the table that the distribution of simulated log-returns is wider (i.e., more spread out) in the bivariate model than in the univariate model for the FTSE series under all scenarios, while this is generally not the case for the S&P series, with the exception of scenario (d). A natural explanation for this is that in the bivariate model the spillover of jumps from the S&P 500 index to FTSE 100 is much more pronounced than vice versa, while the jump size parameters imply on average more negative jump sizes under the univariate specification than under the bivariate model for S&P. Scenario (d) assumes a large asymmetry in the level of intensities, with the intensity for S&P set to the base rate, showing that although the cross-excitation from FTSE to S&P is four times smaller than the reverse cross-excitation, its effect becomes important in this scenario.

Wider distributions imply larger values of standard risk measures used for risk capital calculations such as Value-at-Risk (VaR) and Expected Shortfall (ES). To illustrate, translated into 10-days Value-at-Risk capital requirements at the 99% probability level, the effect of accounting for cross-excitation by the bivariate model, using stress scenarios similar to those in the Global Financial Crisis, implies a risk capital increase from about 6 to 9 cents for each dollar invested in the FTSE 100 index. This can be seen from panel (e), column (2) in Table 6, as $1 - \exp(-0.0661) \approx 6\%$ and $1 - \exp(-0.0889) \approx 9\%$.

We also notice that the distribution of the simulated S&P 500 returns is wider than

that of the FTSE 100 in all scenarios except for scenario (d), due in part to the strong self-excitation of jumps in S&P. Furthermore, the median returns on the S&P 500 are substantially larger than on the FTSE 100 in the asymmetric scenarios except for scenario (d), although the expected number of jumps in the S&P 500 is larger. This result is likely to be driven by the jump risk premia embedded in the expected returns under the physical measure. In other words, there are more jumps expected for the S&P 500, for which investors demand a larger premium to bearing this jump risk. In Appendix D.2.1, we re-compute the results of Table 6 using parameter estimates from the first half of the sample, in which we observe even more pronounced jump contagion asymmetry.

In addition to Table 6, we provide the contour plots for the model with and without cross-excitation, employing a stress scenario induced by a shock in the S&P 500 index, in Figure 3. We observe that the presence of cross-excitation in the bivariate model substantially increases the joint probability of large negative returns in both indices, compared to the situation where cross-excitation is absent (and hence the dependence is driven by the Brownian correlation only). To further analyze the statistical and economic importance of jump contagion, we consider in Appendices D.2.2–D.2.3 two additional applications: (i) prices of multi-index options, and (ii) implied volatility dynamics, for S&P and FTSE. We find there e.g., that the strongest effects of jump contagion on multi-index option prices and implied volatility dynamics for the pair S&P-FTSE occur when mimicking a typical stress scenario that starts off in the US—the leading economy in this pair.

6 Conclusion

We have explored jump contagion in the laboratory of option markets. We have proposed a multivariate option pricing model to capture contagious propagation of jumps among international stock market indices. We have developed an estimation procedure exploit-

Figure 3: Contour plots, with $\lambda_{1,0} = 20, \lambda_{2,0} = \overline{\lambda}_2, h = 10$

(a) Bivariate estimates

(b) Univariate estimates
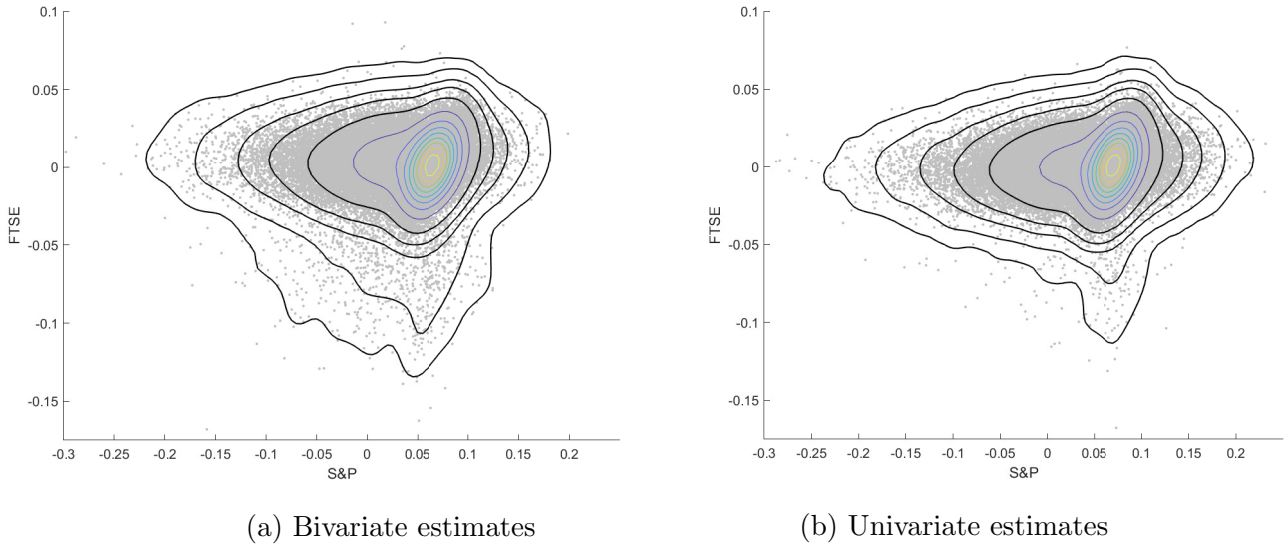
Note: Contour plots overlayed on top of scatter plots of log-return data simulated using parameter estimates for the bivariate model (panel (a)) and the two univariate models (panel (b)). Return horizon set to $h = 10$ days. Initial jump intensities set to $\lambda_{1,0} = 20$ for S&P 500 and $\lambda_{2,0} = \overline{\lambda}_2$ for FTSE 100. Volatilities are assumed to be constant throughout the horizon and are set to $v_{i,s} = 8.36\%$ for both indices, and the instantaneous correlation between Brownian increments is set to be 0.6.

ing the model's conditional characteristic function. This characteristic function depends upon latent stochastic volatilities and jump intensities, and we use it both for backing out stochastic jump intensities from option prices and for the construction of a GMM criterion function based on a continuum of moments. To achieve robust identification, we have followed a semi-parametric approach, replacing spot volatilities with jump-robust realized measures obtained from high-frequency index returns. In addition, to reduce the computational complexity which increases rapidly with the dimension of the system, we have introduced a partial-information approach to implied-state continuum-of-moments GMM estimation, and established its asymptotic properties. Monte Carlo simulations have been conducted to assess the finite-sample behavior.

We have estimated the bivariate specification of our model to carefully synchronized option panels from three pairs of major international stock market indices: FTSE 100, DAX 30, and S&P 500. Our empirical results reveal the presence of significant jump contagion in these option markets. Although these contagion effects are bi-directional in

all index pairs, they are partially asymmetric, with the UK being more affected by the US and Germany than the other way around, and with the US on par with Germany. Finally, we have illustrated the importance of jump contagion for risk management, option pricing, and scenario analysis. Here we find that jump contagion is both statistically and economically relevant, with particularly strong effects in situations where the cross-excitation is asymmetric and the jump intensity in the leading economy is markedly larger than in the other economy.

References

Aït-Sahalia, Y., Cacho-Diaz, J., & Laeven, R. J. (2015). Modeling financial contagion using mutually exciting jump processes. *Journal of Financial Economics*, *117*(3), 585–606.

Aït-Sahalia, Y., Laeven, R. J., & Pelizzon, L. (2014). Mutual excitation in Eurozone sovereign CDS. *Journal of Econometrics*, *183*(2), 151–167.

Aït-Sahalia, Y., & Lo, A. W. (1998). Nonparametric estimation of state-price densities implicit in financial asset prices. *The Journal of Finance*, *53*(2), 499–547.

Aït-Sahalia, Y., & Xiu, D. (2016). Increased correlation among asset classes: Are volatility or jumps to blame, or both? *Journal of Econometrics*, *194*(2), 205–219.

Andersen, T. G., Fusari, N., & Todorov, V. (2017). Short-term market risks implied by weekly options. *The Journal of Finance*, *72*(3), 1335–1386.

Andersen, T. G., Fusari, N., & Todorov, V. (2020). The pricing of tail risk and the equity premium: Evidence from international option markets. *Journal of Business & Economic Statistics*, *38*(3), 662–678.

Bakshi, G., Carr, P., & Wu, L. (2008). Stochastic risk premiums, stochastic skewness in currency options, and stochastic discount factors in international economies. *Journal of Financial Economics*, *87*(1), 132–156.

Bardgett, C., Gourier, E., & Leippold, M. (2019). Inferring volatility dynamics and risk premia from the S&P 500 and VIX markets. *Journal of Financial Economics*, *131*(3), 593–618.

Bollerslev, T., & Todorov, V. (2011). Estimation of jump tails. *Econometrica*, *79*(6), 1727–1783.

Boswijk, H. P., Laeven, R. J., & Lalu, A. (2015). *Asset returns with self-exciting jumps: Option pricing and estimation with a continuum of moments* (Tech. Rep.). Amster-

dam: University of Amsterdam and Tinbergen Institute.

Broadie, M., Chernov, M., & Johannes, M. (2007). Model specification and risk premia: Evidence from futures options. *The Journal of Finance*, *62*(3), 1453–1490.

Carrasco, M., Chernov, M., Florens, J.-P., & Ghysels, E. (2007). Efficient estimation of general dynamic models with a continuum of moment conditions. *Journal of Econometrics*, *140*(2), 529–573.

Carrasco, M., & Florens, J.-P. (2000). Generalization of GMM to a continuum of moment conditions. *Econometric Theory*, *16*(6), 797–834.

Carrasco, M., & Florens, J.-P. (2002). *Efficient GMM estimation using the empirical characteristic function* (Tech. Rep.). Toulouse: Institut d'Économie Industrielle (IDEI).

Du, D., & Luo, D. (2019). The pricing of jump propagation: Evidence from spot and options markets. *Management Science*, *65*(5), 2360–2387.

Duffie, D., Pan, J., & Singleton, K. (2000). Transform analysis and asset pricing for affine jump-diffusions. *Econometrica*, *68*(6), 1343–1376.

Dungey, M., Erdemlioglu, D., Matei, M., & Yang, X. (2018). Testing for mutually exciting jumps and financial flights in high frequency data. *Journal of Econometrics*, *202*(1), 18–44.

Errais, E., Giesecke, K., & Goldberg, L. R. (2010). Affine point processes and portfolio credit risk. *SIAM Journal on Financial Mathematics*, *1*(1), 642–665.

Hawkes, A. G. (1971). Spectra of some self-exciting and mutually exciting point processes. *Biometrika*, *58*(1), 83–90.

Hull, J. C. (2021). *Options, Futures, and Other Derivatives* (11th ed.). Pearson.

Jacod, J., & Todorov, V. (2009). Testing for common arrivals of jumps for discretely observed multidimensional processes. *The Annals of Statistics*, *37*(4), 1792–1838.

Kokholm, T. (2016). Pricing and hedging of derivatives in contagious markets. *Journal of Banking & Finance*, *66*, 19–34.

Medvedev, A., & Scaillet, O. (2007). Approximation and calibration of short-term implied volatilities under jump-diffusion. *The Review of Financial Studies*, *20*(2), 427–459.

Medvedev, A., & Scaillet, O. (2010). Pricing American options under stochastic volatility and stochastic interest rates. *Journal of Financial Economics*, *98*(1), 145–159.

Ogata, Y. (1988). Statistical models for earthquake occurrences and residual analysis for point processes. *Journal of the American Statistical Association*, *83*(401), 9–27.

Pan, J. (2002). The jump-risk premia implicit in options: Evidence from an integrated time-series study. *Journal of Financial Economics*, *63*(1), 3–50.

Singleton, K. J. (2001). Estimation of affine asset pricing models using the empirical characteristic function. *Journal of Econometrics*, *102*(1), 111–141.